 doi:10.20944/preprints202204.0135.v1

Article

Research of active RC- and RLC-filters based on concentrated elements in the basis of ultra-wideband cascades with a minimum number of transistors and low current consumption

Titov A.E.[1], Budyakov P.S.[2], Bugakova A.V.[3], Prokopenko N.N.[3]

[1] South Federal University, Taganrog, Russia
[2] LLC "INNOCENTER VAO", Moscow, Russia
[3] Don State Technical University, Rostov-on-Don, Russia

*E-mail: annabugakova.1992@gmail.com. ORCID: 0000-0001-9255-0015

Abstract: The article shows that active RC- and RLC- filters based on the simplest wideband SiGe transistor stages are quite promising for RF and microwave frequency ranges. The results of computer simulation of the RC- and RLC-filters proposed by the authors of this article, which are oriented for use in communication and telecommunications devices, incl. with tunable and adaptive parameters.

Keywords: Bandpass filters, microwave, EHF, wideband transistor stages

---

1. Introduction

The difficulties of using traditional methods for constructing frequency selection devices stimulate the search for new ways to implement high-frequency RC- and RLC-filters. In this regard, it is promising to switch to signal processing not on the basis of voltages, but on the basis of currents. Circuits operating in the current basis have lower resistance values at the nodes. Therefore, the maximum voltage values at the internal nodes of the circuit in the current basis are much less than when processing signals in the voltage basis. This leads to a decrease in non-linear distortion, expansion of the dynamic range. In addition, parasitic capacitances are charged to lower voltage values, which increases the speed of signal processing and increases the frequency range. However, an appropriate element base is necessary for designing circuits operating in the current basis. Today, the main circuit element in the basis of currents is the so-called current conveyor, which has several generations of development [1-3].

The analysis shows that active RC-filters based on ultra-wideband transistor stages and current amplifiers with a transfer coefficient close to unity have a high potential in the microwave range and, first of all, with restrictions on current

 doi:10.20944/preprints202204.0135.v1

consumption in a static mode. In 2017, analog RC-filters (ARCFs) studies on single transistors at the University of Calgary (Canada) [4-10], as well as articles [11-14], showed that prospects have active filters on single microwave transistors or on the simplest single-stage (two-stage) operational amplifiers (OpAmps).

The purpose and novelty of this article is the computer simulation of ARCFs on wideband cascades with a minimum number of transistors, which makes it possible to designate the areas of their practical application in communication and telecommunications devices.

2. Microwave bandpass ARCF

An example of the implementation of a selective amplifier [15] based on SiGe bipolar transistors in cascode connection is shown in Fig. 2.1.

In this circuit, the frequency of the pole

$$f_p = \frac{1}{2\pi\sqrt{C_1 C_2 R_1 (R_2 + h_{11.1})}} \;, \qquad (1)$$

where $h_{11.1}$ is the low-signal parameter of the *i*-th transistor in the circuit with a common base, is the current gain.

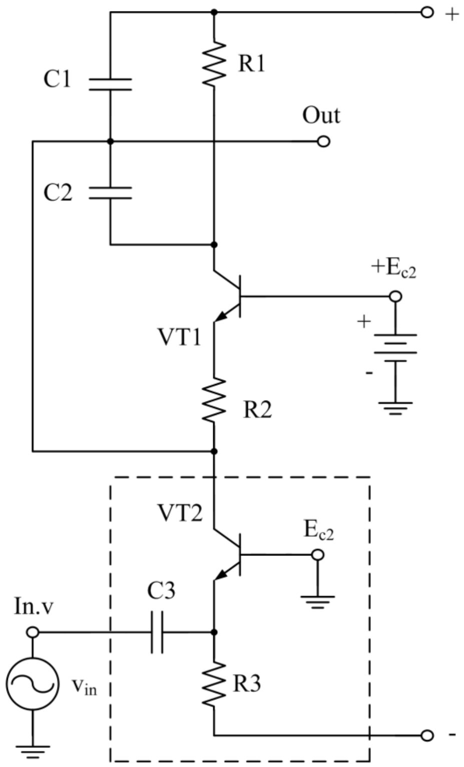

Figure 2.1 The Microwave Bandpass RC-Filter Unit.

Here, the realized quality factor is determined by the formula

Preprints (www.preprints.org) | NOT PEER-REVIEWED | Posted: 14 April 2022 doi:10.20944/preprints202204.0135.v1

$$Q = \left[2\sqrt{m} + \frac{1-\alpha_1}{\sqrt{m}}\right]^{-1}, \qquad (2)$$

where $m = (R_2 + h_{11.1})/R_1$.

At

$$m = \frac{R_2 + h_{11.1}}{R_1} = \frac{1-\alpha_1}{2} \qquad (3)$$

the maximum quality factor of the pole is equal to

$$Q_{max} = \frac{\sqrt{(1+\beta_1)}}{2\sqrt{2}}, \qquad (4)$$

where $\beta_1 = \alpha_1/(1-\alpha_1)$ is the current gain of the base of the transistor VT1.

However, in any case, the circuit gain at the pole frequency f_p is determined by the following relationship:

$$K_0 = Q\frac{\alpha_2}{h_{11.2}}\sqrt{R_1(R_2 + h_{11.1})}\sqrt{k}\ , \qquad (5)$$

where $k = C_1/C_2$.

To simplify the procedure for cascading such a unit in the input circuit of the circuit, an isolation capacitor C3 is used. The exclusion of its influence on the above parameters requires the fulfillment of the inequality:

$$C_3 \gg \frac{\frac{1}{R_3} + \frac{1}{h_{11.2}}}{2\pi f_p}\ . \qquad (6)$$

Fig. 2.2 shows a circuit schematic of the microwave RC-filter Fig. 2.1, and Fig. 2.3 presents the results of its simulation in Agilent ADS CAD based on SiGe 0.25 μm technology (SG25H1 manufacturing process).

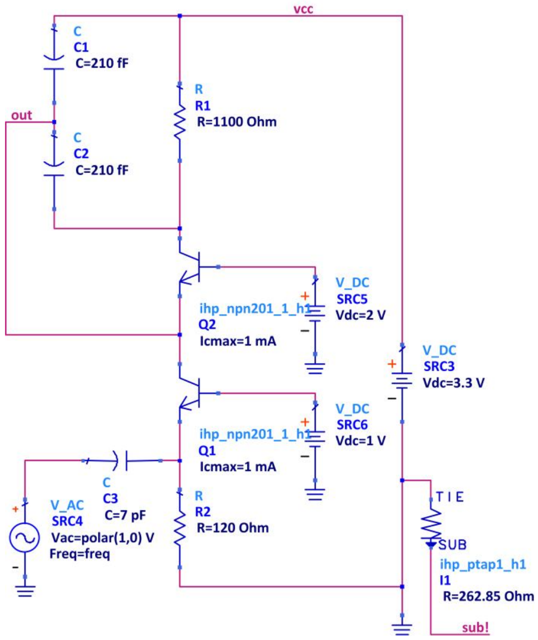

Figure 2.2 The RC-Filter Unit Circuit in ADS Environment.

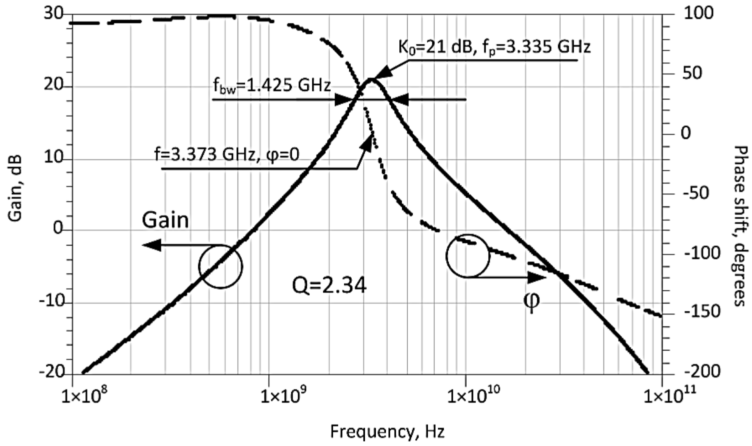

Figure 2.3 The Amplitude and Phase-Frequency Characteristics of the Active Microwave Filter Unit in Fig. 2.2.

3. EHF Bandpass RLC-Filter

In the bandpass filter structure, integral low-Q inductances can be used while maintaining the basic properties of the frequency-setting circuit.

Fig. 3.1 shows a variant of the implementation of such a circuit in the structure of a selective amplifier based on a current follower implemented on a transistor VT1.

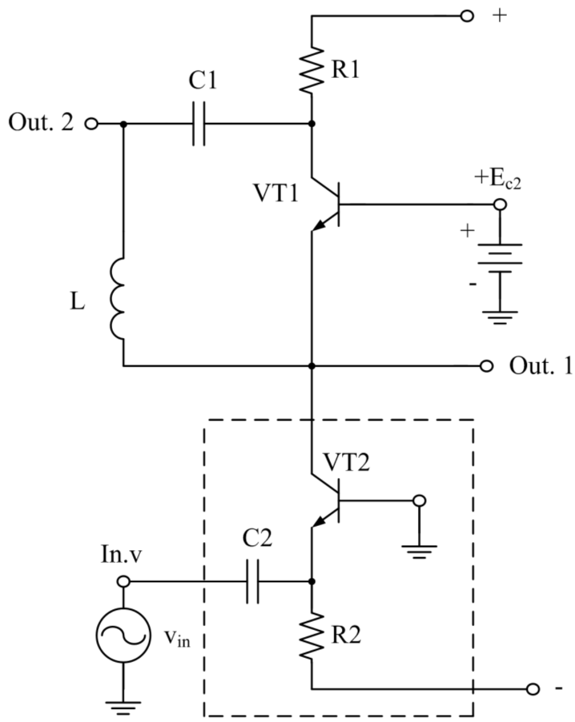

Figure 3.1 The Selective RLC-Amplifier of the EHF Range.

Preprints (www.preprints.org) | NOT PEER-REVIEWED | Posted: 14 April 2022 doi:10.20944/preprints202204.0135.v1

Here:

- pole frequency

$$f_p = \frac{1}{2\pi\sqrt{LC}}\ , \qquad (7)$$

- quality factor of the pole

$$Q = \sqrt{\frac{L}{C}}/[h_{11.1} + R(1 - \alpha_1)]. \qquad (8)$$

As can be seen from (8), the ratio of C and L determines the value of Q. The "advantage" realized by the circuit depends on the quality factor of the pole of the circuit. For example, with L=10 nH, R=R1=100 Ohm, C=10 fF and a current consumption of 1 mA, we get that GHz; Q=37. Therefore, the influence of the high-frequency parameters of the transistor on both f_p and Q decreases by almost two orders of magnitude in comparison with the classical RC-unit.

In addition, in the version of the RLC-amplifier, it is possible to adjust the realizable quality factor of the pole with virtually no change in f_p. Indeed, as follows from (8), a change in the input resistance VT1 ($h_{11.1} = f(I_0)$) under the action of the static emitter current (I_0) affects Q.

Fig. 3.2 shows a diagram of a second-order EHF RLC-unit in Agilent ADS, and Fig. 3.3 presents the results of its simulation based on SiGe 0.25 μm technology (SG25H1 process technology [16]).

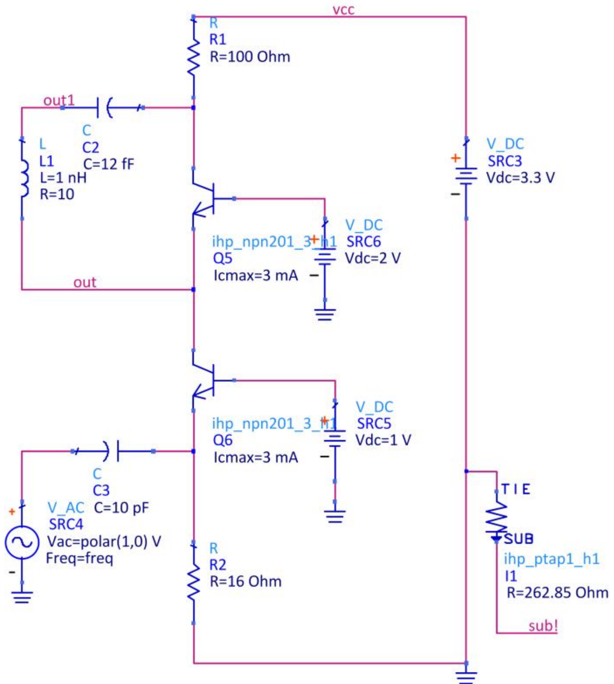

Figure 3.2 The EHF RLC-Filter in ADS Environment.

Preprints (www.preprints.org) | NOT PEER-REVIEWED | Posted: 14 April 2022 doi:10.20944/preprints202204.0135.v1

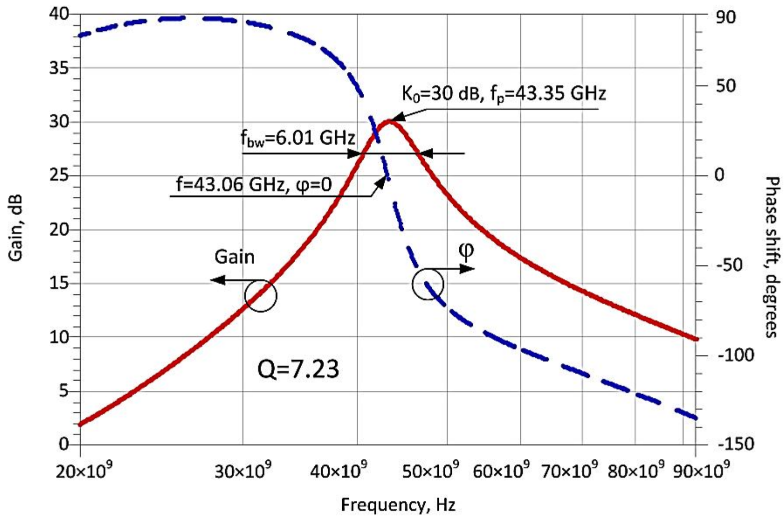

Figure 3.3 The Simulation Results of the RLC-Filter in Fig. 5.

In contrast to the microwave range, in the EHF range, a special parametric optimization of the circuit is needed, taking into account the influence of other high-frequency effects not considered here.

4. Bandpass filter with a non-inverting current amplifier implemented on n-p-n transistors

The proposed bandpass filter circuit (BPF, Fig. 4.1) contains two transistors VT1, VT2, as well as the classic current mirror CM1, implemented on n-p-n transistors. The low frequency OpAmp A1, although not required, can be used to stabilize the static mode and achieve zero output voltage. The transistor VT2 provides increased input impedance of the BPF.

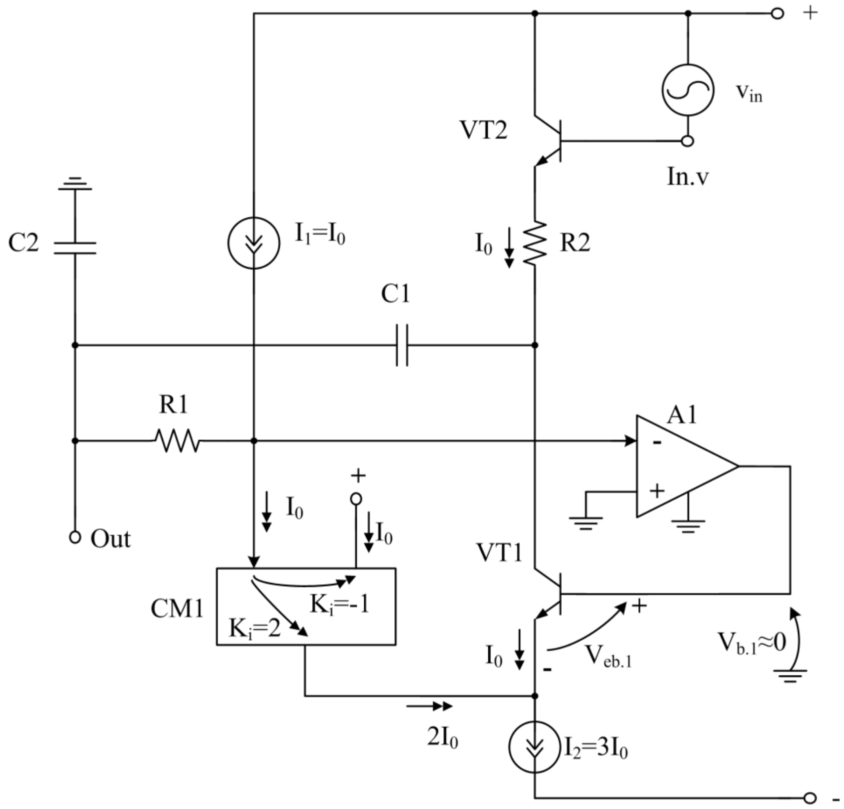

Figure 4.1 The Bandpass Filter with a Non-Inverting Current Amplifier CM1, Implemented on n-p-n Transistors.

The feature of the circuit in Fig. 4.1 consists in the fact that the operational amplifier A1 provides a low level of the constant component at the output of the ARCF and practically does not affect the operation of the ARCF in the high frequency range.

Modeling the circuit in Fig. 4.1 was made in the MicroCap environment (Fig. 4.2, Fig. 4.3).

 doi:10.20944/preprints202204.0135.v1

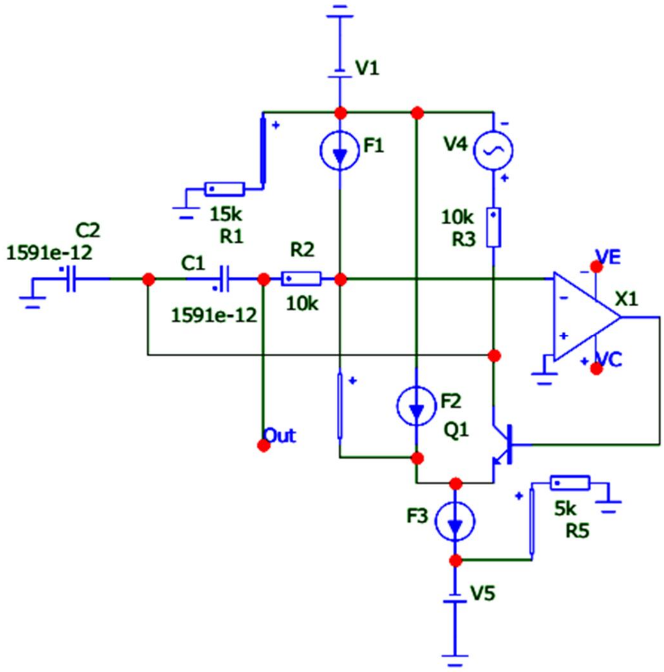

Figure 4.2 The BPF Circuit (Fig. 4.1) in the MicroCap Environment.

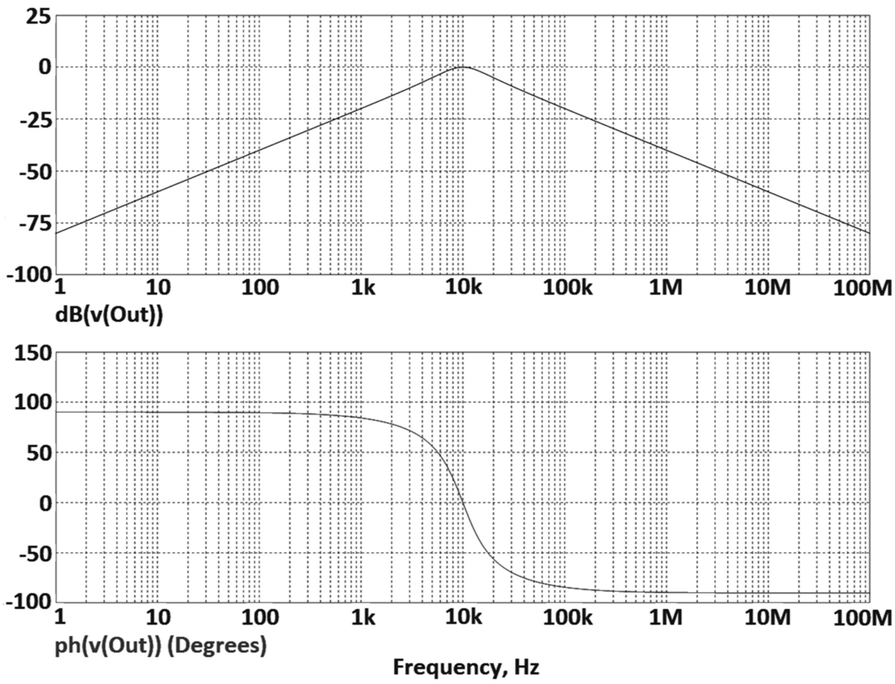

Figure 4.3 The Amplitude-Frequency and Phase-Frequency Characteristics of the Filter in Fig. 4.2.

The parameters of the frequency setting elements must have different values for a higher frequency range.

Preprints (www.preprints.org) | NOT PEER-REVIEWED | Posted: 14 April 2022 doi:10.20944/preprints202204.0135.v1

5. Microwave bandpass filter on bipolar p-n-p transistors

The proposed filter circuit in Fig. 5.1 contains the current mirror CM1, the cascode amplifier VT1 and the potential bias circuit VT2. Due to this, the constant component at the output of ARCF is close to zero. The input signal is relative to the negative rail of the power supply.

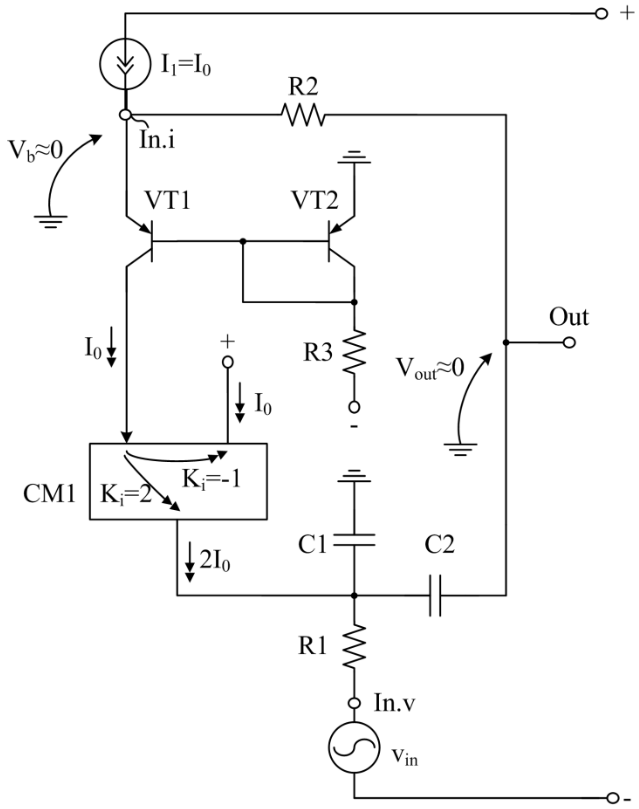

Figure 5.1 Circuit of the Microwave Bandpass Filter on p-n-p Transistors.

Modeling the circuit of Fig. 5.1 was made in the MicroCap environment (Fig. 5.2, Fig. 5.3).

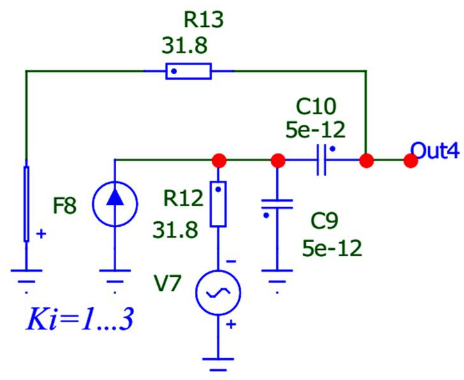

Figure 5.2 The Bandpass Filter in Fig. 5.1 in MicroCap Environment.

 doi:10.20944/preprints202204.0135.v1

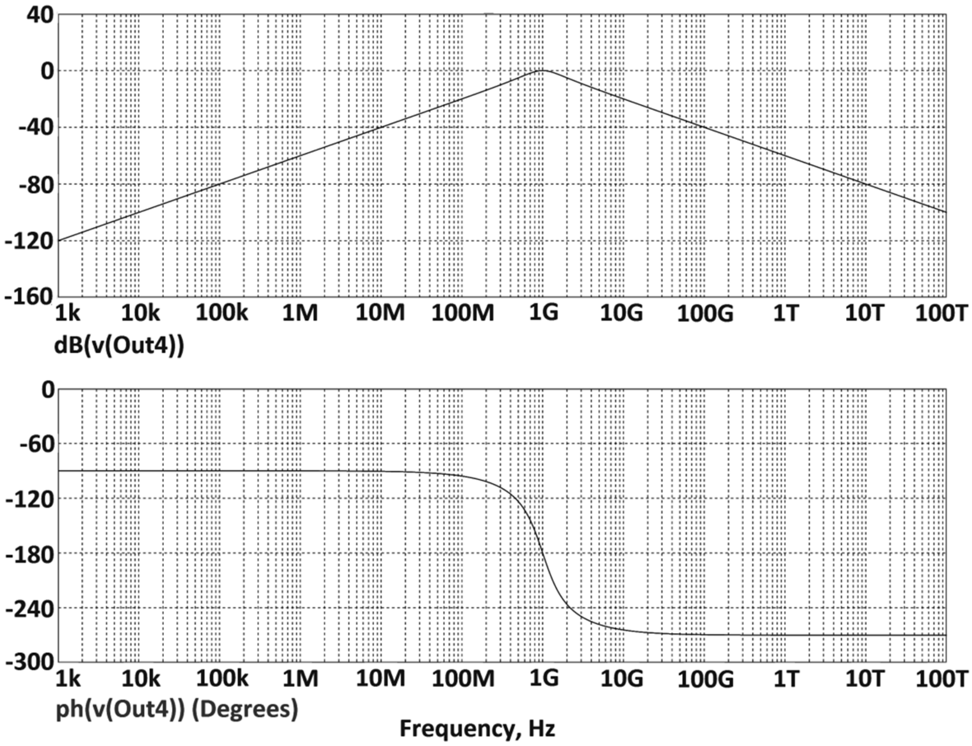

Figure 5.3 The Amplitude-Frequency and Phase-Frequency Characteristics of the Bandpass Filter in Fig. 5.2.

Analysis of the graphs in Fig. 5.2 shows that with the selected parameters of the elements, the pole frequency f_p=1GHz is provided, as well as good attenuation of the signal in the microwave range (-40dB at f_p=100GHz).

6. Selective amplifier based on SiGe n-p-n transistors of SGB25VD process technology

The proposed circuit of the BPF in Fig. 6.1 includes transistors VT1 and VT3, as well as a current mirror (VD1, VT2) with a current transfer coefficient greater than one. This mode is provided by the parallel connection of several transistors in the VT2 structure.

Preprints (www.preprints.org) | NOT PEER-REVIEWED | Posted: 14 April 2022 doi:10.20944/preprints202204.0135.v1

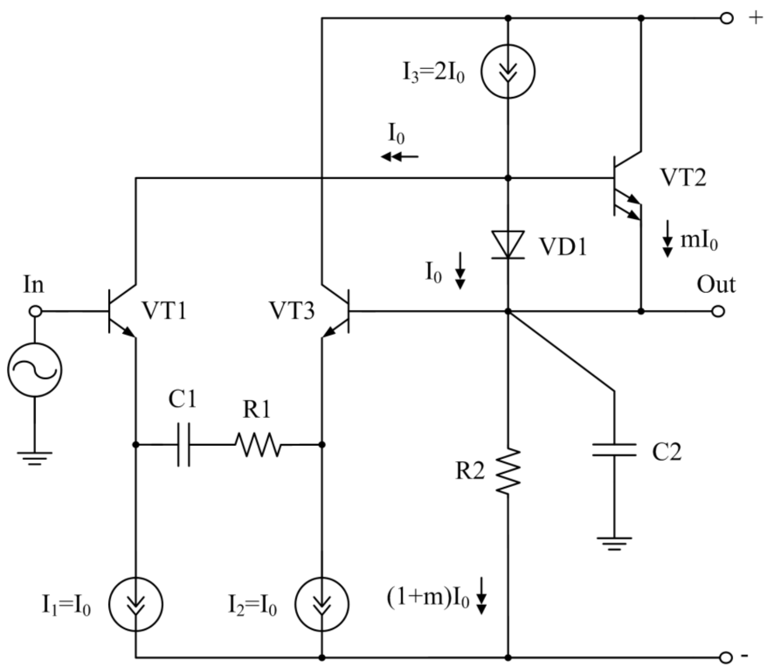

Figure 6.1 The Circuit of the Selective Amplifier on n-p-n Transistors.

Modeling of the selective amplifier was carried out in the ADS environment (Fig. 6.2).

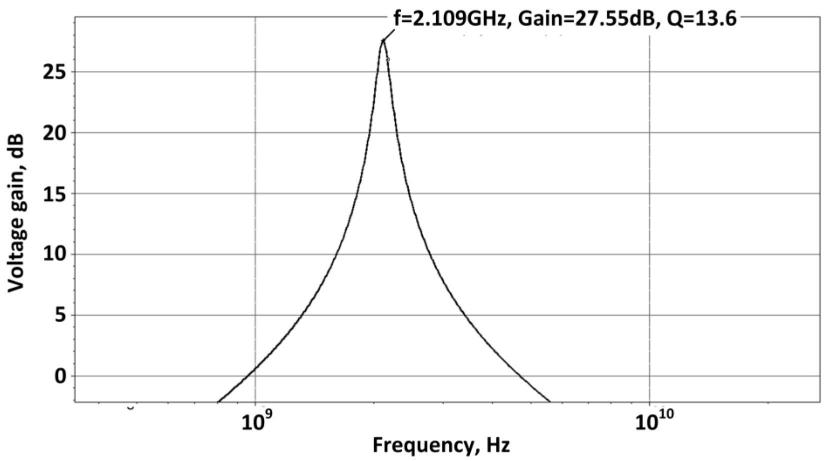

Figure 6.2 The Logarithmic Amplitude-Frequency Characteristic of the BPF Gain in Fig. 6.1.

7. Low-voltage selective amplifier based on complementary bipolar transistors

In the proposed BPF in Fig. 7.1 frequency setting elements are C1, R1 and C2, R2. The feature of this circuit is the parallel connection of several transistors in

Preprints (www.preprints.org) | NOT PEER-REVIEWED | Posted: 14 April 2022 doi:10.20944/preprints202204.0135.v1

the structure of the VT3 three-terminal network, which provides a current gain of the current mirror of more than one.

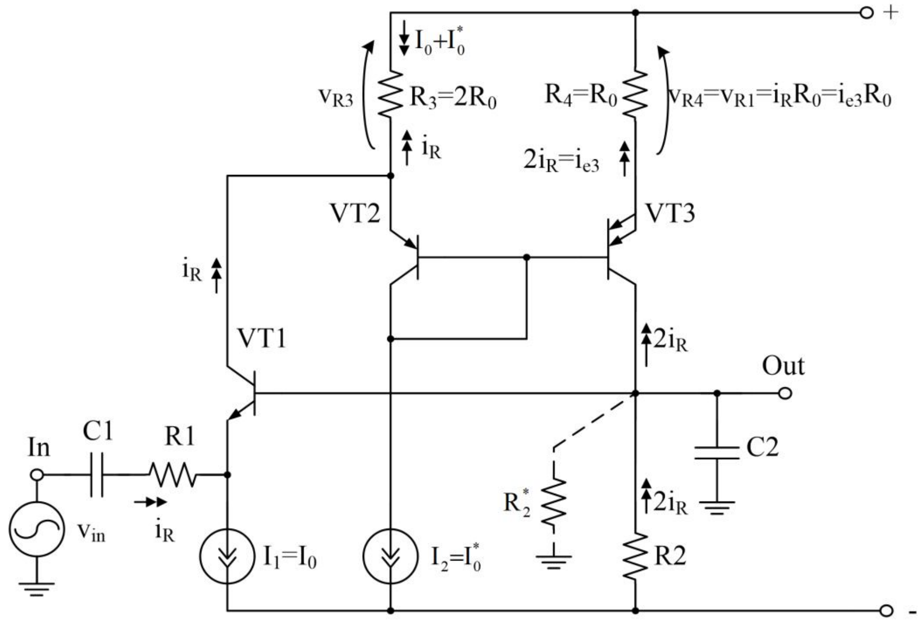

Figure 7.1 The Bandpass Filter on Complementary Bipolar Transistors.

Modeling of the selective amplifier in Fig. 7.1 was made in the ADS environment (Fig. 7.2).

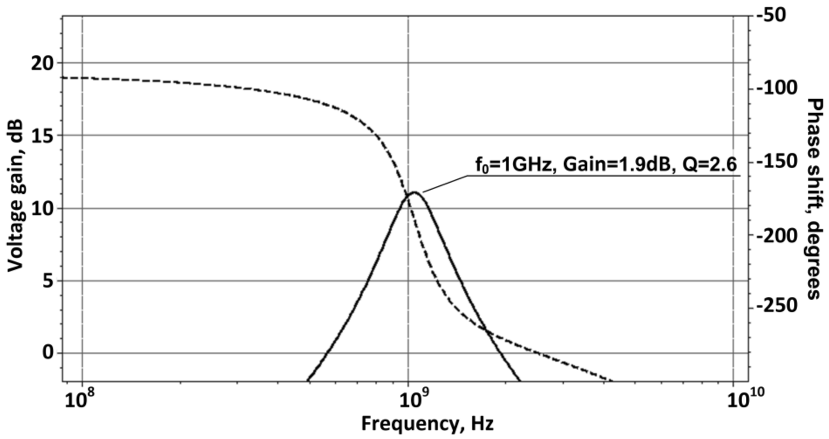

Figure 7.2 The Logarithmic Amplitude-Frequency and Phase-Frequency Characteristics of the BPF in Fig. 7.1.

8. Controlled bandpass RC filter based on the Gilbert amplifier

The use of the Hilbert amplifier in the BPF circuit in Fig. 8.1 allows us to change the filter parameters by controlling the static mode of transistors VT2, VT3.

Preprints (www.preprints.org) | NOT PEER-REVIEWED | Posted: 14 April 2022 doi:10.20944/preprints202204.0135.v1

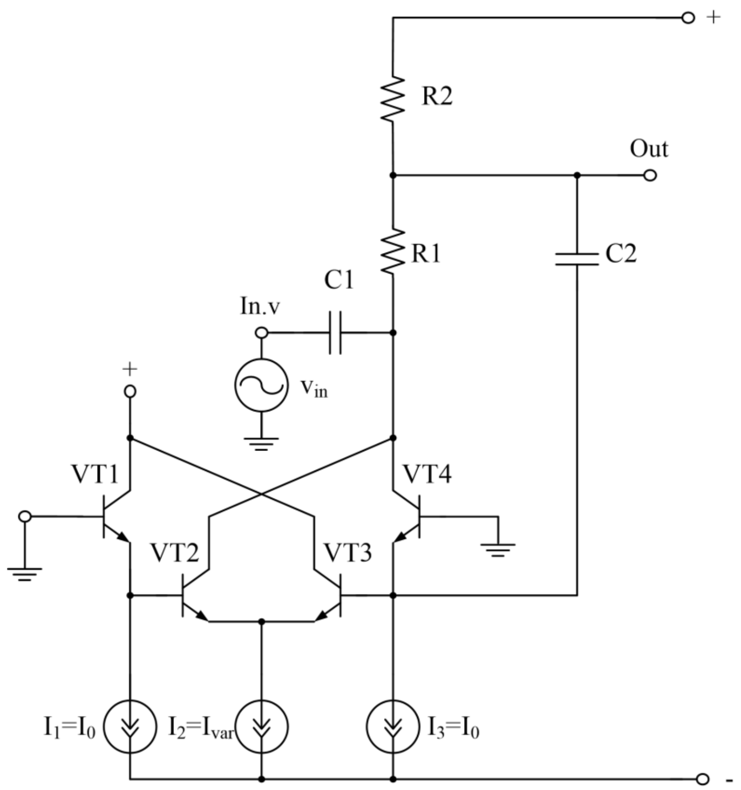

Figure 8.1 The Controlled RC-Filter Based on the Gilbert Amplifier.

The amplitude-frequency characteristic of the filter at various currents I_2=I_{var} is shown in Fig. 8.2.

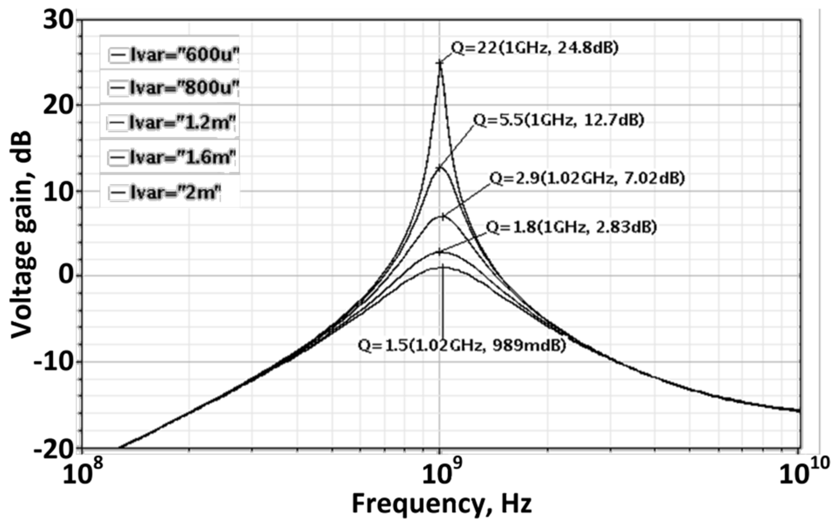

Figure 8.2 The Logarithmic Amplitude-Frequency Characteristic of the bandpass filter in Fig. 8.1 at different current values I_2=I_{var}.

Thus, the control of the quality factor of the pole and the gain at a constant pole frequency of 1 GHz is provided in the circuit in Fig. 8.1.

Conclusion

The considered circuit design of bandpass filters based on the simplest SiGe broadband transistor stages is quite promising for the RF and microwave frequency ranges. At the same time, low current consumption is ensured and the high-frequency properties of transistors are effectively used. Application of SiGe technology, incl. technological processes SG25H1, SG25RH allows to ensure the operation of ARCF in the range of low temperatures, as well as in conditions of penetrating radiation.

The research has been carried out at the expense of the Grant of the Russian Science Foundation (project No. 18-79-10109-P).

References

1. F. Yu, P. Li, L. Gao, S. Cai, K. Gu and W. Wang, "A Second Generation Current Controlled Current Conveyor Realization Using Cascode Current Mirror : A CCCII Realization Using Cascode Current Mirror," 2018 10th International Conference on Communications, Circuits and Systems (ICCCAS), Chengdu, China, 2018, pp. 29-33. doi: 10.1109/ICCCAS.2018.8769163
2. V. Vijay, "Second generation differential current conveyor (DCCII) and its applications, " GRIN Verlag, 2020, 134 p.
3. R. Senani, D. R. Bhaskar and A. K. Singh, "Current Conveyors: Variants, Applications and Hardware Implementations, " Springer International Publishing, Switzerland, 2015 DOI 10.1007/978-3-319-08684-2
4. B. J. Maundy *et al.*, "Single transistor RC-only second-order allpass filters, " International Journal of Circuit Theory and Applications, 2020, vol. 48, no. 2, pp. 162-169.
5. M. B. Elamien, B. J. Maundy, L. Belostotski and A. S. Elwakil, "Wideband third order single transistor all-pass filter", Int J Circ Theor Appl., vol. 48, pp. 1201-1208, 2020.
6. N. N. Poddar, "Design and Implementation of Single Transistor Active Filters (Unpublished master's thesis), " University of Calgary, Calgary, AB. doi:10.11575/PRISM/25573 http://hdl.handle.net/11023/3538
7. M. B. Elamien, B. J. Maundy, L. Belostotski and A. S. Elwakil, "Low-Power Single-Transistor Voltage-Mode Third-Order All-pass Filter in 65-nm CMOS," 2020 IEEE 63rd International Midwest Symposium on Circuits and Systems

(MWSCAS), Springfield, MA, USA, 2020, pp. 1-4. doi: 10.1109/MWSCAS48704.2020.9184478
8. M. B. Elamien, B. J. Maundy, L. Belostotski, and A. S. Elwakil, "Wideband third-order single-transistor all-pass filter," International Journal of Circuit Theory and Applications, vol. 48, no. 7, pp. 1201-1208, 2020. doi: 10.1002/cta.2786
9. M. B. Elamien, B. J. Maundy, L. Belostotski, and A. S. Elwakil, "An ultra-low power wide-band single-transistor second-order allpass filter in 65nm cmos, " in 2019 IEEE 62nd International Midwest Symposium on Circuits and Systems (MWSCAS), pp. 373–376, IEEE, 2019. doi:10.1109/mwscas.2019.8885329
10. B. J. Maundy, A. S. Elwakil, L. Belostotski, and N. Herencsar, "Single transistor rc-only second-order allpass filters, " International Journal of Circuit Theory and Applications, vol. 48, no. 2, pp. 162–169, 2020. doi:10.1002/cta.2721
11. S. R. Aghazadeh, H. Martinez, A. Saberkari, "5GHz CMOS all-pass filter-based true time delay cell, " Electronics, 2019, vol. 8, no. 1, pp. 16.
12. L. Pantoli, V. Stornelli, "Filter Design Solutions for RF systems, " Electronics, MDPI, 2020, 186 p.
13. L. C. Severo, W. M. A. Van Noije, "ULV and ULP Operational Amplifiers for Active-RC Filters, " Ultra-low Voltage Low Power Active-RC Filters and Amplifiers for Low Energy RF Receivers, Springer, Cham, 2022,pp. 11-31. doi: 10.1007/978-3-030-90103-5_2
14. L. C. Severo and W. Van Noije, "A 10.9-μW/pole 0.4-V active-RC complex BPF for Bluetooth low energy RF receivers," 2018 IEEE 9th Latin American Symposium on Circuits & Systems (LASCAS), Puerto Vallarta, Mexico, 2018, pp. 1-4. doi: 10.1109/LASCAS.2018.8399975
15. N. N. Prokopenko, S. G. Krutchinsky, M. N. Makhmudov, P. S. Budyakov, " Microwave Selective Amplifier, " Patent RU No. 2519006, February 10, 2014. (In Russian)
16. "Parameter section of SiGe:C BiCMOS process technology, " [Online]. Available: http://www.ihp-microelectronics.com/services/research-and-prototyping-service/mpw-prototyping-service/sigec-bicmos-technologies